Desktop 3D Printer Material Properties and Dimensional Accuracy

Garrett W. Melenka[1], Jonathan S. Schofield[1], Michael R. Dawson[2], Dr. Jason P. Carey[1]

[1]*Mechanical Engineering, Faculty of Engineering, University of Alberta, Edmonton Alberta T6G 2G8, Canada*

[2]*Glenrose Rehabilitation Hospital, Edmonton, Alberta, Canada, T6G 2E1*

Corresponding Author E-mail: jpcarey@ualberta.ca

Abstract

Three dimensional (3D) printing is a rapidly expanding manufacturing method. Initially, 3D printing was used for prototyping but now this method is being employed to create functional final products. In recent years, desktop 3D printers have become commercially available to academics and hobbyists as a means of rapid component manufacturing. Although these desktop printers are able to facilitate reduced manufacturing times, material costs and labor costs; relatively little literature exists to quantify the physical properties of the printed material as well as the dimensional consistency of the printing processes. This paper evaluates the material properties and dimensional accuracy of a MakerBot Replicator II desktop 3D printer. A design of experiments (DOE) test protocol was applied to determine the effect of the following variables on the material properties of 3D printed part: layer height, percent infill and print orientation. DOE results suggest that percent infill has a significant effect on the longitudinal elastic modulus and ultimate strength of the test specimens whereas print orientation and layer thickness failed to achieve significance. Dimensional analysis of test specimens shows that the test specimen varied significantly ($p<0.05$) from the nominal print dimensions. Although desktop 3D printers are an attractive manufacturing option to quickly produce functional components, this study suggests

users must be aware of this manufacturing process' inherent limitations, especially for components requiring high geometric tolerance or specific material properties. Therefore, higher quality 3D printers and more detailed investigation into the MakerBot MakerWare printing settings are recommended if consistent material properties or geometries are required.

Introduction

Three Dimensional Printing

Three Dimensional (3D) printing is a manufacturing technique that produces components or assemblies from computer aided design (CAD) software. 3D printing technology was originally developed to create prototypes and deemed too expensive for final products; however, with the recent introduction of several inexpensive desktop printers, this is changing. Potential applications include biomedical engineering that require customization, low volume production runs, or part geometry difficult to obtain with traditional subtractive methods (Leigh et al. 2012, Murr et al. 2010, Gibson et al. 2006). For example, Fused Deposition Modeling manufacturing methods have been used for bioresorbable scaffold structures for bone tissue (Hutmacher et al. 2001, Zein et al. 2002). 3D printing is being integrated into orthopedic and oral/ maxillofacial reconstructions (Gibson et al. 2006).

3D printing is divided into four main manufacturing methods: Stereolithography (SLA), Laminated Object Manufacturing (LOM), Selective Laser Melting (SLM), and Fused Deposition Modeling (FDM) (Hull 1986, Chua, Leong & Lim 2003, Crump 1989, Novakova-Marcincinova, Novak-Marcincin 2013) .

Desktop 3D printing, designed for home as well as academic use, is a rapidly growing industry. Most desktop 3D printers use FDM, which deposits extruded molten plastic filament from a nozzle comprised of resistive heaters. The extruded plastic cools and hardens on the machine build plate. Parts are built through successive deposition of plastic filament layers. Examples of FDM –based desktop 3D printers

include the RepRap®, Fab@Home and Makerbot 3D printers; these can be purchased for less than US$2300 (Malone, Lipson 2007). Desktop 3D printers use acrylonitril butadiene styrene (ABS) or polylactic acid (PLA) thermoplastics feedstock. Conversely, industrial 3D printers, by companies such as Objet and Z Corporation, may cost over US$50,000 (Chua, Leong & Lim 2003) . Material properties and precision of industrial 3D printers have been studied (Pilipovic, Raos & Šercer 2009) , but not those of desktop 3D printers.

As the build resolution of the MakerBot Replicator ll is not stated, nor has a reliable method for determining properties been presented by the manufacturer, this study will investigate dimensional print consistency and material properties of printed tensile samples and assess the printer as a viable final product-manufacturing tool. A design of experiments (DOE) testing protocol will evaluate test samples as done previously by Ahn, to evaluate FDM printing of ABS samples material properties (Ahn et al. 2002). Three variables that are readily manipulated using Makerbot's print software were identified (layer height, print orientation and infill percentage) and will be the subject of our DOE strength and elastic modulus study.

Methods

Test samples were printed using a MakerBot Replicator II desktop printer (MakerBot Industries, Brooklyn USA) with 1.75mm diameter polylactide (PLA) filament available through Makerbot Industries. Print parameters were specified and controlled using MakerWare 2.2.0 control software (MakerBot Industries, Brooklyn USA). The MakerBot Replicator II is limited to printing with PLA filament.

Table 1 provides layer thickness resolution and stepper motor positioning precision of the Makerbot Replicator II printer (Anonymous2013a) . Build resolution for the MakerBot Replicator ll is not stated by the manufacturer.

Table 1: MakerBot Replicator II layer and positioning precision

Layer Resolution Settings	High	100 µm
	Medium	270 µm
	Low	340 µm
Positioning Precision	XY	11 µm
	Z	2.5 um

The dimensions and general geometry of the ASTM test samples are shown in Table 2 and Figure 1, respectively (Anonymous2010) . Test samples were designed using a computer aided design (CAD) software package (SolidWorks 2013 SP4.0, Dassault Systems, Vélizy-Villacoublay, France CAD files were converted into a stereolithography file (STL) and imported into the MakerWare software. MakerWare software was used to control the printer settings such as layer height, percent infill, print orientation and extruder speed. Finally, an .x3g file was exported to the MakerBot Printer to generate the 3D part. All manipulated variables for the test samples were controlled using the MakerWare software.

Table 2: Dimensions of tensile specimen

Geometry (Figure 1)	**Dimensions (mm)**
Total Length (L)	113.45
Length of Narrow Section (LN)	33
W = Width of Ends (W)	25
Width of Narrow portion (WN)	6.2
Transition Radius Outside (TRO)	14
Transition Radius Inside (TRI)	25
Thickness (TN)	2

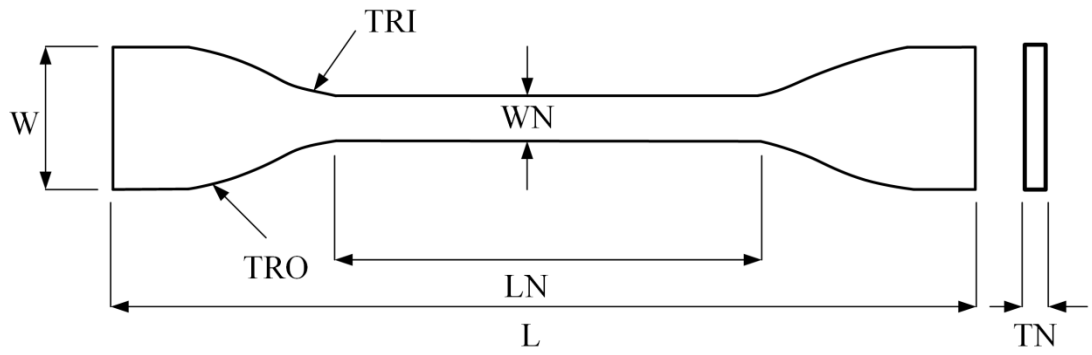

Figure 1: Shape of test specimen for tensile testing W- width, WN- width narrow section L-length, TN-thickness, LN-length of narrow section, TRO- transition radius outside, TRI- transition radius inside

An MTS Tensile testing machine (Synergy 400, Material Testing Solutions, Eden Prairie, USA), shown in Figure 2, with a 500-N load cell was used to perform tensile tests on samples. Samples were tested until failure at a loading rate of 500 mm/s (Anonymous2010) . TestWorks Software (Material Testing Solutions, Eden Prairie, USA) sampling at 500 Hz captured load and extension data. Stress was calculated by dividing the measured load by the sample narrow section cross-sectional area (WN by TN). Strain was computed through measuring the change in length of the sample, as measured from the tensile machine stroke. Strain was computed by dividing stroke by LN. Samples were tested in random order.

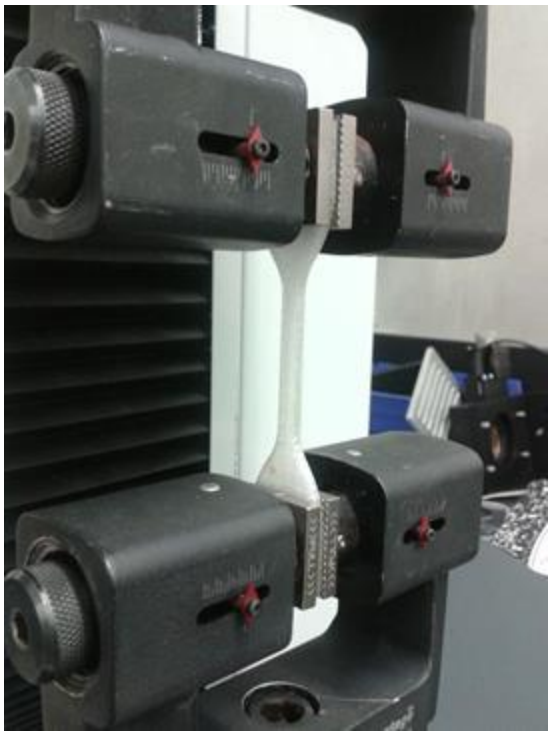

Figure 2: MTS Synergy 400 experimental setup to evaluate test specimen material properties

Design of Experiments Analysis

DOE was selected to determine which of the selected variables, percent infill, layer thickness and print orientation, had a significant effect on sample longitudinal elastic modulus and tensile strength. The variables percent infill and print orientation are comparable to the air gap and orientation of raster variables used by Ahn *et al*. Layer print height (layer height) was evaluated at 0.1 and 0.25 mm thickness, print orientation at 45 and 90 degrees (Figure 3) and print infill (PI) at 10, 45 and 80 percent.

When manufacturing the test samples the following control variables were used:

- Extruder temperature (230 °C)
- Extruder Head Speed (90 mm/s)
- Number of Shells (2)
- One sample was printed at a time
- same filament spool

Analysis was performed using a DOE 2^3 full factorial analysis with percent infill mid points with a total of 32 test samples (Table 3). Samples 1-8 in Table 3 show the factor combinations for the 2^3 full factorial analysis. Samples 9-12 represent the mid-points used to assess if non-linearities exist for infill percentage variable. Three replicates were performed for each combination of variables, an additional two replicates were performed to evaluate the infill percentage midpoints. This analysis quantified the significance of each variable on maximum stress and elastic modulus, and accounted for two-way interactions between variables.

Maximum stress for each sample was that which was recorded from the TestWorks software given the samples initial cross sectional area it was identified using the MAX command in Excel (Microsoft Office Excel 2003, Microsoft Corp. Redmond, Washington, USA). Longitudinal elastic modulus is the slope of initial elastic deformation region of the stress-strain data for each sample collected by TestWorks; it was determined using linear regression in Excel.

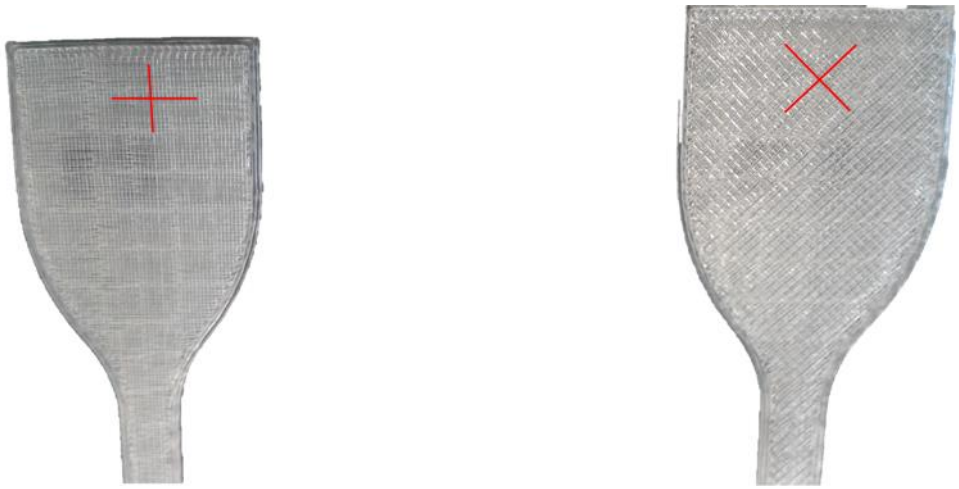

(a) (b)

Figure 3: Print orientation (a) 90 degree orientation (b) 45 degree orientation

Table 3: Test matrix to evaluate the material properties of PLA printer test specimen

Sample	Number of	Layer	Print	Infill

	Replicates	Height (mm)	Orientation (degrees)	(percent)
1	3	0.10	45	10
2	3	0.10	45	80
3	3	0.10	90	10
4	3	0.10	90	80
5	3	0.25	45	10
6	3	0.25	45	80
7	3	0.25	90	10
8	3	0.25	90	80
9	2	0.10	45	45
10	2	0.10	90	45
11	2	0.25	45	45
12	2	0.25	90	45

Statistical analysis was performed using Statistica 10 (StatSoft, Tulsa, OK). In addition to the DOE analysis, the variable combination that yielded the highest maximum stress values was printed four additional times and tested to failure to evaluate production repeatability. Mean and standard deviation values for both longitudinal elastic modulus and maximum stress were calculated.

Test Sample Geometric Analysis

Sample geometric consistency was evaluated. Overall dimensions of the each sample (**Figure 1**) were verified using a digital caliper (0–150mm ± 10 µm, digital caliper, Mastercraft Tool Company, Earth City, USA). The WN, TN, L and W dimensions were measured for comparison with the dimensions defined in the CAD software. Mean and standard deviation values for these dimensions were calculated, as well as a one sample student's t-test performed to evaluate significant differences ($p<0.05$). An unpaired two tailed t-test was conducted on thickness values to evaluate if a significant difference existed in sample thicknesses printed in layer thicknesses of 0.10 mm compared to 0.25mm ($p<0.05$).

Analytical Elastic Constants

The elastic constants for the FDM tensile specimen were calculated using classical laminate plate theory (CLPT) (Tsai, Hahn 1980) and using the unidirectional elastic constants for FDM (Rodríguez, Thomas & Renaud 2003) . The test specimen fabricated using the MakerBot Replicator II 3D printer forms a laminate structure due to the nature of the FDM printing method. The laminate structure of the 3D printed test samples and the print orientation can be seen in Figure 3. The equations for the unidirectional representative element (RVE) are shown in Equation **Error! Reference source not found.** - 5).

$$E_{11} = (1 - p_1)E \tag{1}$$

$$E_{22} = (1 - p_1^{1/2})E \tag{2}$$

$$G_{12} = G\frac{(1 - p_1)(1 - p_1^{1/2})}{(1 - p_1) + (1 - p_1^{1/2})} \tag{3}$$

$$\upsilon_{12} = (1 - p_1)\upsilon \tag{4}$$

$$\upsilon_{21} = (1 - p_1^{1/2})\upsilon \tag{5}$$

where E, G and v represent the elastic modulus, shear modulus and Poisson's ratio for PLA extruded plastic (Table 3). E_{11} and E_{22} represent the lamina longitudinal and transverse elastic modulus for the two dimensional FDM laminate and G_{12} represent the in-plane shear modulus, v_{12} and v_{21} are the major and minor Poisson's ratio for the 2D laminate and p_1 represents the void density for each lamina. The void density range used in this study ranged from 20-90%, which corresponds to 80 and 10% infill.

Table 4: Elastic properties of polylactic acid plastic (Anonymous2013c)

Material Property	Value
Elastic Modulus- *E* (GPa)	3.5
Shear Modulus- *G* (GPa)	2.4
Poisson's Ratio- *v*	0.366

A micromechanical model will be used to calculate the laminae properties. The properties are then transformed to account for the print angle of the laminae. The unidirectional stiffness matrix, transformation matrix and transformed stiffness matrices are shown in equation (6) -(8).

$$[Q]=\begin{bmatrix} \frac{E_{11}}{1-\upsilon_{12}\upsilon_{21}} & \frac{E_{11}\upsilon_{21}}{1-\upsilon_{12}\upsilon_{21}} & 0 \\ \frac{E_{11}\upsilon_{21}}{1-\upsilon_{12}\upsilon_{21}} & \frac{E_{22}}{1-\upsilon_{12}\upsilon_{21}} & 0 \\ 0 & 0 & G_{12} \end{bmatrix} \tag{6}$$

$$[T]=\begin{bmatrix} \cos^2\theta & \sin^2\theta & 2\sin\theta\cos\theta \\ \sin^2\theta & \cos^2\theta & -2\sin\theta\cos\theta \\ -\sin\theta\cos\theta & \sin\theta\cos\theta & \cos^2\theta-\sin^2\theta \end{bmatrix} \tag{7}$$

$$\overline{Q}=[T]^{-1}[Q][T]^{-T} \tag{8}$$

Laminate elastic modulus of the sample, E_{xx}, is determined from CLPT analysis from:

$$E_{xx}=\frac{1}{a_{11}t} \tag{9}$$

where a_{11} is the first term of the inversed stiffness matrix

$$\begin{bmatrix} A & B \\ B & D \end{bmatrix}^{-1}=\begin{bmatrix} a & b \\ b & d \end{bmatrix} \tag{10}$$

Where the A, B, and D matrices are computed for the entire laminate using the following equations:

$$A=\sum_{k=1}^{n}\left(\overline{Q}\right)\left(z_k-z_{k-1}\right) \tag{11}$$

$$B=\frac{1}{2}\sum_{k=1}^{n}\left(\overline{Q}\right)\left(z_k^2-z_{k-1}^2\right) \tag{12}$$

$$D=\frac{1}{3}\sum_{k=1}^{n}\left(\overline{Q}\right)\left(z_k^3-z_{k-1}^3\right) \tag{13}$$

In equation (11)), n represents the number of lamina in the laminate, z_k represents the lamina thickness and $\overline{Q}$ is the transformed stiffness matrix for each lamina. The thickness of the entire laminate is denoted as *t*. In this study the analytical laminate stacking sequences were $[90 / 0]_{10}$ and $[45/-45]_{10}$ and $[90 / 0]_4$ and $[45/-45]_4$ for the 0.1mm and 0.25mm samples respectively.

The test sample cross-section is shown in Figure 4 where the sample consists of two areas: exterior shell structure and interior laminate structure. The exterior shell structure defines the FDM part shape and contains only solid PLA. To account for the exterior shell structure on the test specimen material properties, an area weighted elastic modulus will calculated.

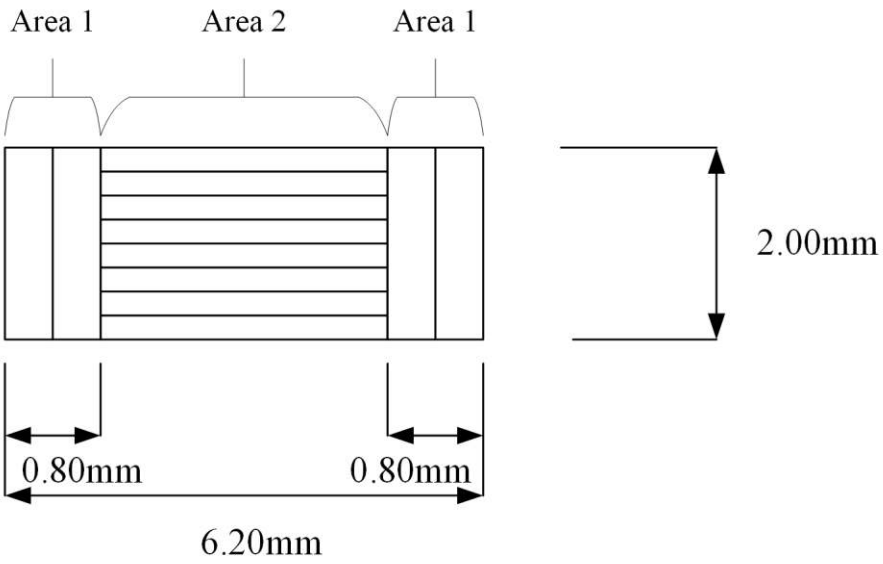

Figure 4: Test sample cross-section schematic. Area 1 exterior shell structure Area 2 internal laminate structure

The area weighted elastic modulus will be calculated using the following equation:

$$E = \frac{E_{shell}A_1 + E_{laminate}A_2}{A_{total}} \tag{14}$$

where E_{shell} is the shell elastic modulus and $E_{laminate}$ is the laminate elastic modulus calculated using above CLPT method. The external shell will consist of isotropic PLA material. Each shell is 0.4mm thick.

Results

Design of Experiments Analysis

The significance of infill percentage, layer height and print orientation, to longitudinal elastic modulus was quantified as well as interaction effects between these variables. As infill percentage included testing at three levels (10%, 45% and 80%), linear and quadratic effects were examined. The linear effect of infill percentage was determined to have the only significant effect on longitudinal elastic modulus (p<0.05) (Table 5). Although not statistically significant, the main layer height demonstrated the second greatest effect (Table 5). Interactions between variables showed no significant effect on sample longitudinal elastic modulus.

Table 5: Longitudinal elastic modulus effects-estimates. Highlighted row indicates statistically significant variables. infill % –PI, Layer Height-LH, Print orientation- PO.

			Confidence Limits		
	Effect	Standard Error	-95%	+95%	P-Value
Mean / Interaction	1064.78	14.89	1033.89	1095.67	<0.01
PO	42.36	29.79	-19.42	104.14	0.170
IP (Linear)	262.16	33.78	192.11	332.21	<0.01
IP (Quadratic)	20.61	33.78	-49.44	90.66	0.550
LH	-57.76	29.79	-119.54	4.02	0.065
PO X IP (Linear)	-21.16	33.78	-91.21	48.89	0.537
PO X IP (Quadratic)	-12.12	33.78	-82.17	57.93	0.723
PO X LH	22.11	29.25	-38.56	82.77	0.458
IP (Linear) X LH	-26.30	33.78	-96.35	43.75	0.445
IP (Quadratic) X LH	50.45	33.78	-19.61	120.50	0.150

Since interactions of the main effects demonstrated no significant influence on longitudinal elastic modulus, a reduced statistical model was adopted that ignored interaction effects as a means of further evaluating the significance of the main effects. When distinguished from the effects of interactions, both

linear infill percentage and layer height significantly affected longitudinal modulus (Table 6). Yet, in context, the linear effect of infill percentage has a much greater effect. From Table 6 this effect is approximately 4 times that of layer height.

Table 6: Reduced longitudinal elastic modulus effects estimates. Highlighted row indicates statistically significant variables. infill % –PI, Layer Height-LH, Print orientation- PO.

			Confidence Limits		
	Effect	Standard Error	-95%	+95%	P-Value
Mean / Interaction	1065	14.596	1034.833	1094.73	<0.01
PO	44.38	28.666	-14.434	103.201	0.133
IP (Linear)	262.2	33.001	194.246	330.079	<0.01
IP (Quadratic)	20.61	33.001	-47.303	88.53	0.538
LH	-66.2	28.666	-124.983	-7.347	0.0289

When evaluating the individual main effects, it is possible to see that print orientation demonstrates relatively large standard deviation while showing minimal change in longitudinal elastic modulus between the 45 and 90 degree print orientations (Figure 5 (a)). Layer height did demonstrate significance, and it is possible to see that the longitudinal elastic modulus at 0.1mm layer height can be expected to be greater than the 0.25 mm layer height (Figure 5 (b)). Finally, infill percentage demonstrates the greatest change in longitudinal elastic modulus across its range (10%, 45% and 80%) (Figure 5 (c)). This variable also demonstrates notably smaller standard deviations at each level and as a result develops the greatest significance of the three variables.

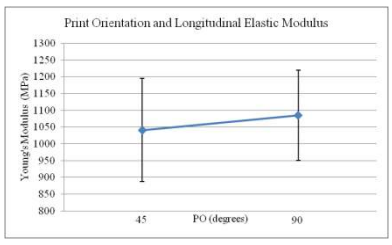

(a)

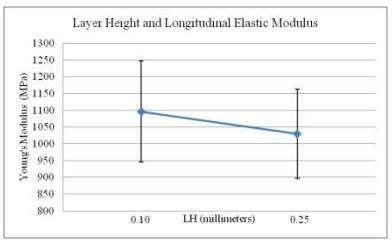

(b)

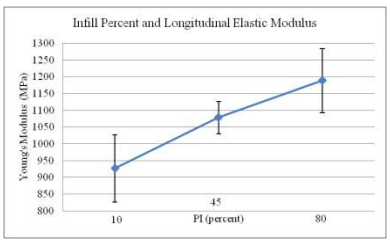

(c)

Figure 5: Mean plots for elastic modulus

The significance, with relation to maximum stress, of the three variables as well as interaction effects between these variables was quantified. Similar to the elastic modulus procedure, infill percentage included testing at three levels (10%, 45% and 80%) and both linear and quadratic effects were considered in the results. Again, the linear effect of Infill percentage was the only significant effect on maximum stress (p<0.05) (Table 7).

When quantifying the effect on maximum stress, linear infill percentage again has the greatest effect (Table 7). All other variables and interactions showed no significant effect on sample maximum stress.

Table 7: Maximum stress effects estimates. Highlighted row indicates statistically significant variables.

			Confidence Limits		
	Effect	Standard Error	-95%	+95%	P-Value
Mean / Interaction	33.77	0.49	32.75	34.79	<0.01
PO	0.22	0.98	-1.82	2.26	0.822
IP (Linear)	2.45	1.12	0.14	4.76	0.038
IP (Quadratic)	1.31	1.12	-1.01	3.62	0.254
LH	0.19	0.98	-1.85	2.23	0.85
PO X IP (Linear)	0.07	1.12	-2.24	2.38	0.95
PO X IP (Quadratic)	-0.33	1.12	-2.64	1.99	0.771
PO X LH	0.41	0.97	-1.59	2.42	0.673
IP (Linear) X LH	-0.66	1.12	-2.98	1.65	0.558
IP (Quadratic) X LH	-0.4	1.12	-2.72	1.91	0.721

Again, a reduced statistical model was adopted to exclusively evaluate main effects, ignoring variable interactions. In this reduced model, again only linear infill percentage demonstrated statistically

significant effect. Table 8 shows that linear Infill percentage's effect is substantially larger than other variables.

Table 8: Reduced maximum stress effects estimates. Highlighted row indicates statistically significant variables.

			Confidence Limits		
	Effect	Standard Error	-95%	+95%	P-Value
Mean / Interaction	33.77	0.452	32.84	34.69	<0.01
PO	0.28	0.887	-1.54	2.1	0.756
IP (Linear)	2.45	1.025	0.35	4.55	0.024
IP (Quadratic)	1.31	1.025	-0.79	3.41	0.212
LH	0.26	0.887	-1.57	2.08	0.776

When evaluating the individual main effects, it is possible to see the insignificant effects; print orientation and layer height demonstrate relatively large standard deviations while showing minimal change in maximum stress across levels (Figure 6 (a) and (b)). Infill percentage demonstrated a significant effect on maximum stress across its range (Figure 6 (c)). This variable also demonstrates notably smaller standard deviations at each level with exception of 10% infill samples.

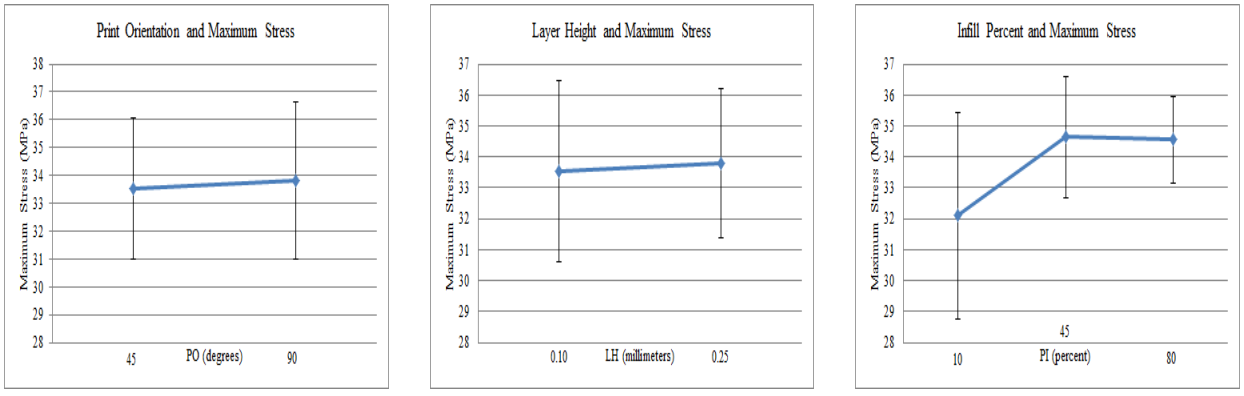

(a) (b) (c)

Figure 6: Mean plots for maximum stress

Test sample dimensional accuracy

All samples are expected to have dimensions similar to the nominal solid model dimensions. The comparison of the measured tensile sample dimensions to the nominal dimension is summarized in Table 9. An unpaired t-test was used to compare the nominal tensile dimensions with the measured dimensions with a *p*-value of < 0.05 indicating that a statistically significant difference exists. Table 9 shows that there was a statistically significant difference for all dimensions of the tensile samples from the nominal dimensions.

Table 9: Comparison of MakerBot geometry with nominal dimensional values

	Length (L)	Width (W)	Width Narrow (WN)	Thickness Narrow (TN)
Nominal Measurement (mm)	113.45	25.00	6.20	2.00
Actual Measurement Average (mm)	112.86	25.03	6.30	2.12
Actual Measurement Standard Deviation (mm)	0.12	0.07	0.06	0.10
Percent Error (%)	0.51	0.13	1.71	6.05
p-value	<0.001	0.015	<0.001	<0.001

Analytical Elastic Constants

The effective longitudinal elastic modulus was computed for the three manipulated variables used in this study using the CLPT analysis method. The resulting longitudinal elastic constants are shown in Table 10. The 0.1mm layer thickness samples had the following laminate stacking sequences: $[90 / 0]_{10}$ and $[45/-45]_{10}$ and the 0.25mm layer thickness had the following stacking sequence $[90 / 0]_4$ and $[45/-45]_4$. The average longitudinal elastic modulus from the DOE analysis is also included in Table 10.

Table 10: Analytical and experimental elastic constants for 3D printed PLA. SD: standard Deviation.

Elastic Modulus (GPa)				
	1	2	3	4

Layer Thickness (mm)	CLPT	DOE (SD)	CLPT	DOE (SD)	CLPT	DOE (SD)	CLPT	DOE (SD)
0.1	2.66	1.24 (0.06)	1.10	0.99 (0.15)	2.45	1.26 (0.07)	1.05	0.93 (0.06)
0.25	2.66	1.17 (0.07)	1.10	0.94 (0.09)	2.45	1.09 (0.10)	1.05	0.85 (0.07)
1-	80 % infill and [90 / 0] stacking sequence							
2-	10% infill and [90/0] stacking sequence							
3-	80 % infill and [45 / -45] stacking sequence							
4-	10% infill and [45/-45] stacking							

Discussion

Design of Experiments Analysis

Infill percentage was determined to have the largest effect on the elastic modulus of the samples. When evaluating main effects it was also possible to see that layer height has a statistically significant, yet minor, impact on elastic modulus. Both infill percentage and layer height (Figure 5) demonstrate relatively high standard deviations when compared to infill percentage (Figure 5 (c)). These larger standard deviations ultimately reduce the significance of these variables. It is possible that these two variables actually exhibit a stronger effect on elastic modulus however inconsistencies in the printing process inhibited the ability to sufficiently quantify these relationships.

Infill percentage demonstrated the only significant effect on maximum stress when evaluating both interactions and main effects (Table 7). Similar to the longitudinal elastic modulus analysis both layer height and print orientation demonstrated relatively high standard deviations. As a result the statistical significance of layer height and print orientation was reduced. Again, it is possible these two parameters may have demonstrated significance, yet inconsistencies in the printing process, or unforeseen confounding factors may have inhibited this. At 10% infill the

standard deviation demonstrated was larger than at 45% and 80% (Figure 6 (c)). This finding can perhaps be attributed to the physical lack of material in the infill and resulting unpredictability with reduced presence of material.

The experimental design called for three replicates of each sample, ultimately strengthening the statistical power of the analyses. Yet, in both longitudinal elastic modulus and maximum stress, the data presented high standard deviations. The large deviations can be attributed to inconsistencies and unforeseen confounding factors associated with the printing process. The study by Ahn et al. showed that print orientation has a significant effect on material properties. This result was not found in this study. The lack of significance for the print orientation could be attributed to the print shells which define the test specimen shape.

Test sample dimensional accuracy

The MakerBot Replicator ll 3D printer can achieve 100 μm layer thicknesses but build resolutions in the x-axis, y-axis or z axis directions are not stated by the manufacture. By comparison professional desktop 3D printers such as the Objet30 Pro (Anonymous2013b) can achieve the following print resolutions:

Table 11: Objet30 Pro build resolutions (Anonymous2013b)

Specifications	Objet30 Pro
Layer thickness	28 μm
Build Resolution X-axis	600 dpi
Build Resolution Y-axis	600 dpi
Build Resolution Z-axis	900 dpi
Accuracy	0.1 mm

As build resolution of the Makerbot Replicator is not stated an evaluation of the test sample geometry was necessary to determine if components can be repeatedly and reliably manufactured.

The dimensional analysis of the tensile samples has shown that significant differences between the original CAD dimensions and final printed component dimensions exist.

Analytical Elastic Constants

Elastic constants determined experimentally and through the CLPT analysis both demonstrate that the elastic modulus for the PLA printed samples are less than the isotropic elastic PLA modulus shown in Table 4. This shows that the FDM printed parts should not be treated as isotropic materials.

Analysis of the theoretical elastic constants demonstrated that layer print height does not affect the elastic properties of the laminated samples whereas print orientation and infill have an effect over the elastic modulus. Layer height was investigated in this study since this parameter is one of the primary print parameters in the MakerWare software for creating 3D parts. However, layer height affects print quality and should be taken into account when constructing a part.

A substantial difference exists between the elastic modulus of the 10% and 80% infill printed parts. Print orientation also has an effect on the longitudinal elastic modulus however; the difference between elastic modulus for parts printed with [90 / 0] and [45/-45] orientations is not as great as the difference between the 80 and 10% infill samples. The experimental DOE results in Table 10 followed a similar trend to the theoretical CLPT results. The 80% infill components had a greater longitudinal elastic modulus than the 10% infill components. As well, the [90 / 0] print orientation parts had a greater elastic modulus than the [45/-45] parts.

The experimental results for the tensile samples demonstrated similar trends to the analytical model for the FDM manufactured parts. The experimental results show that infill creates a significant difference in the elastic modulus. The experimental results also show that layer height has a significant effect on elastic modulus when a reduced model is used however; the significance of the layer height is

much less than that of the percent infill. The CLPT results demonstrate that the elastic modulus should be independent of layer thickness. The experimental analysis showed that layer thickness has a significant effect on elastic modulus. The experimental result for layer thickness may be attributed to the dimensional accuracy of the 3D printer. Table 9 shows that the average sample thickness was 2.12 ± 0.1 mm, therefore layer thicknesses of 0.1 and 0.25mm were not achieved during sample printing. Variations in layer thickness from the expected values would result in changes to the sample elastic modulus.

The DOE testing of the tensile samples did not yield as large a difference between the longitudinal elastic modulus for the 80% and 10% in fill samples as the CLPT theoretical results predict. The difference between the theoretical model and experiments may be due to voids inherent to the FDM printing process. Periodic voids along the shell and infill boundary are shown in Figure 7. The existence of voids along the shell-infill interface will cause a decrease in test sample strength.

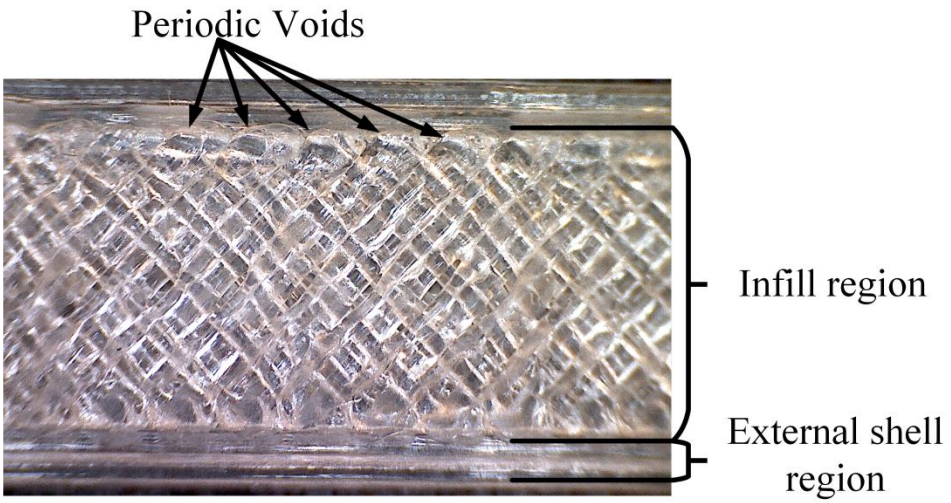

Figure 7: Periodic voids along the shell and infill boundary occurring in a [45/-45] tensile sample

The presence of voids along the shell-infill boundary when creating the 3D parts may also account for the inability to resolve a significant difference between the [90 / 0] and [45/-45] print orientations since the voids will obscure the effect of print orientation.

Conclusions

A desktop 3D printer was used in this study to manufacture tensile samples. Tensile tests were performed to quantify the material behavior of the PLA used for sample fabrication. Evaluation of the material properties is necessary if functional parts are to be manufacture using this style of 3D printer. Three variables were selected for a DOE study to determine if these manufacturing parameters have a significant effect on material properties. The DOE study has shown that in-fill has a significant effect on the material properties of the PLA 3D printed parts whereas layer thickness and print orientation were not shown to significantly affect the sample material properties. Therefore in order to maximize part strength it is recommended to use higher levels of infill. This study has shown that components created using the MakerBot Replicator II had significant dimensional variations from the nominal dimensions.

Overall the Makerbot Replicator II printer demonstrates the ability to print relatively low cost components in a short time frame. However, the Makerbot replicator II also demonstrated statistically significant dimensional deviations from the input CAD file geometry. Furthermore, when quantifying maximum stress values and longitudinal elastic modulus values, the tensile samples demonstrated relatively high standard deviations. Undoubtedly, the Makerbot replicator II has the potential to dramatically impact prototype development in a research environment. Designers must be aware of inherent limitations in this technology when designing functional components to tight dimensional tolerances or specific material properties.

Acknowledgments

The authors would like to thank Disha Patel for her help with the printing and testing of the tensile samples and Dr. Ming Chan for the use of his 3D printer.

References

MakerBot Replicator 2 Desktop 3D Printer User Manual 2013a, .

Objet30 Pro Professional Desktop Printer Technical Specifications 2013b, .

, *Overview of materials for Polylactic Acid (PLA) Biopolyme*2013c, [2013, 08/16].

ASTM D638-10 Standard Test Method for Tensile Properties of Plastics 2010, .

Ahn, S.-., Montero, M., Odell, D., Roundy, S. & Wright, P.K. 2002, "Anisotropic material properties of fused deposition modeling ABS", *Rapid Prototyping Journal,* vol. 8, no. 4, pp. 248-257.

Chua, C.K., Leong, K.F. & Lim, C.S. 2003, *Rapid Prototyping : Principles and Applications,* World Scientific, Singapore.

Crump, S.S. 1989, *Apparatus and method for creating three-dimensional objects*.

Gibson, I., Cheung, L.K., Chow, S.P., Cheung, W.L., Beh, S.L., Savalani, M. & Lee, S.H. 2006, "The use of rapid prototyping to assist medical applications", *Rapid Prototyping Journal,* vol. 12, no. 1, pp. 53-58.

Hull, C.W. 1986, *Apparatus for Production of Three-dimensional Objects by Stereolithography*.

Hutmacher, D.W., Teoh, S.H., Zein, I., Ng, K.W., Schantz, J.-. & Leahy, J.C. 2001, "Design and fabrication of a 3D scaffold for tissue engineering bone", *ASTM Special Technical Publication,* , no. 1396, pp. 152-167.

Leigh, S.J., Bradley, R.J., Purssell, C.P., Billson, D.R. & Hutchins, D.A. 2012, "A Simple, Low-Cost Conductive Composite Material for 3D Printing of Electronic Sensors", *PLoS ONE,* vol. 7, no. 11.

Malone, E. & Lipson, H. 2007, "Fab±Home: The personal desktop fabricator kit", *Rapid Prototyping Journal,* vol. 13, no. 4, pp. 245-255.

Murr, L.E., Gaytan, S.M., Medina, F., Lopez, H., Martinez, E., MacHado, B.I., Hernandez, D.H., Martinez, L., Lopez, M.I., Wicker, R.B. & Bracke, J. 2010, "Next-generation biomedical implants using additive manufacturing of complex cellular and functional mesh arrays", *Philosophical Transactions of the Royal Society A: Mathematical, Physical and Engineering Sciences,* vol. 368, no. 1917, pp. 1999-2032.

Novakova-Marcincinova, L. & Novak-Marcincin, J. 2013, *Selected testing for rapid prototyping technology operation*.

Pilipovic, A., Raos, P. & Šercer, M. 2009, "Experimental analysis of properties of materials for rapid prototyping", *International Journal of Advanced Manufacturing Technology,* vol. 40, no. 1-2, pp. 105-115.

Rodríguez, J.F., Thomas, J.P. & Renaud, J.E. 2003, "Mechanical behavior of acrylonitrile butadiene styrene fused deposition materials modeling", *Rapid Prototyping Journal,* vol. 9, no. 4, pp. 219-230.

Tsai, H.C. & Hahn, H.T. 1980, *Introduction to Composite Materials,* Technomic Publishing Co, Westport, CT.

Zein, I., Hutmacher, D.W., Tan, K.C. & Teoh, S.H. 2002, "Fused deposition modeling of novel scaffold architectures for tissue engineering applications", *Biomaterials,* vol. 23, no. 4, pp. 1169-1185.